

# Modeling the Atmospheric Airborne Fraction in a Simple Carbon Cycle Model

F. Terenzi<sup>1\*</sup> and S. Khatiwala<sup>2</sup>

<sup>1</sup>Department of Applied Physics and Applied Mathematics, Columbia University, New York, NY 10027, USA; <sup>2</sup>Lamont–Doherty Earth Observatory, Columbia University, Palisades, NY 10964, USA

14 March 2009

## ABSTRACT

The fraction of anthropogenic CO<sub>2</sub> emissions remaining in the atmosphere, known as the airborne fraction ( $A_F$ ), has remained roughly constant over the last 50 years, averaging about 50–60%. Since  $A_F$  is widely considered a fundamental property of the carbon cycle, its historical constancy has been taken as evidence that anthropogenic emissions have not as yet triggered a “climate-carbon-cycle feedback”. Projections of future atmospheric CO<sub>2</sub> levels and hence climate are often justified on this basis. On the other hand, recent measurements show a slight increase in  $A_F$ , leading some authors to suggest that climate change feedbacks are now becoming significant. However, increases in  $A_F$  are also predicted by complex carbon cycle models, even in the absence of such feedbacks. Thus, it remains unclear how one should interpret the observed historical constancy of  $A_F$ , or its recent trends. Given the importance attributed to  $A_F$ , particularly in formulating climate policy, it is therefore imperative to understand the reason for its long-term constancy, and why it has stabilized around a particular value. A related question is whether a future increase in  $A_F$  necessarily imply the operation of climate-carbon feedbacks. In order to address these questions, we have developed and applied a simple box model of the anthropogenically-perturbed global carbon cycle. We show that our model output is in good agreement with both historical observations and the predictions of far more sophisticated carbon cycle models. We then carry out a series of idealized experiments and find that, rather than being a fundamental property of the carbon cycle,  $A_F$  depends sensitively on both the shape of the emission history and its growth rate. Specifically, our results suggest that both the quasi-constancy of  $A_F$  over the past half-century, and its particular numerical value of  $\approx 50\%$ , are essentially a consequence of exponentially growing emissions with a nearly-constant growth rate of  $\approx (40 \text{ y})^{-1}$ . Furthermore, our results suggest that although we cannot rule out climate-carbon feedbacks, fluctuations in the emission growth rate and/or changes in the absorbing capacities of the ocean and land biosphere, offer plausible, and perhaps simpler, explanations for the recent observed trends in  $A_F$ .

## 1 Introduction

Atmospheric CO<sub>2</sub> mixing ratios depend on the capacity of the ocean and terrestrial biosphere to absorb anthropogenic emissions of CO<sub>2</sub> (Fung *et al.*, 2005). It is estimated that about 40 to 60% of these emissions remain in the atmosphere (Hansen and Sato, 2004; Jones and Cox, 2005), implying that the ocean and the land biosphere absorb approximately half the human-emitted CO<sub>2</sub>. The relationship between the atmospheric increase in CO<sub>2</sub> and emissions has generally been characterized using a parameter known as the “airborne fraction”,  $A_F$ , defined as the ratio of the annual increase of atmospheric CO<sub>2</sub> to total emissions from anthropogenic sources (Forster *et al.*, 2007). Observations show that  $A_F$  has remained roughly constant over the last 50 years (Keeling *et al.*, 1995). One common interpretation of this historical constancy is that  $A_F$ , and its particular observed value, is in some way a fundamental property of the carbon cycle (e.g., Broecker, 1975;

Broecker *et al.*, 1979; Hansen *et al.*, 1981; Siegenthaler and Joos, 1992; Hansen and Sato, 2004). (This interpretation relies on the argument that anthropogenic emissions have not as yet triggered a “climate-carbon-cycle feedback” (Jones and Cox, 2005; Friedlingstein *et al.*, 2006).) Projections of future atmospheric CO<sub>2</sub> levels and hence climate are often predicated on this interpretation (Firor, 1988). For example, Hansen and Sato (2004) use it to predict that the long-term CO<sub>2</sub> growth rate will be 1.9 ppm/year. Recent work by Canadell *et al.* (2007), however, suggests a slight increase in the airborne fraction. According to these authors, this implies that the carbon cycle is generating “stronger-than-expected” and “sooner-than-expected” climate forcing. Increases in  $A_F$  due to climate change feedbacks are also predicted by simulations performed with coupled climate-carbon models, largely due to the negative impact of climate change on land carbon storage (Friedlingstein *et al.*, 2006; Solomon *et al.*, 2007). However, the same suite of models, with the feedbacks switched off also show an upward trend in  $A_F$ . Thus, it remains unclear how one should interpret the observed historical constancy of, or recent trends in,  $A_F$ .

In order to gain insight into this problem, and in particular

\* Corresponding author.  
e-mail: ft2104@columbia.edu

elucidate the factors controlling the airborne fraction, we have developed and applied a simple model of the global carbon cycle. The model comprises of three boxes representing the atmosphere, land-biosphere and ocean. While box models are highly simplified descriptions of the carbon cycle, they offer a very convenient tool for understanding the complex partitioning of carbon among key reservoirs, especially on a global scale. A wide variety of box models of varying degrees of complexity have therefore been developed to study various aspects of the anthropogenically-perturbed carbon cycle (e.g., *Oeschger et al.*, 1975; *Siegenthaler and Oeschger*, 1978; *Sarmiento and Toggweiler*, 1984; *Toggweiler et al.*, 2003a;b). Indeed, the ‘‘Bern model’’, a three-box carbon cycle model (*Siegenthaler and Joos*, 1992; *Joos et al.*, 1996; *Plattner et al.*, 2008), is used by the IPCC (*Houghton et al.*, 2001; *Solomon et al.*, 2007) to generate predictions of atmospheric CO<sub>2</sub> in response to various emission scenarios. (These predictions are then used to force the climate models participating in the IPCC study.) In our model, ocean uptake of anthropogenic CO<sub>2</sub> is represented via a transit-time distribution or Green’s function (*Hall et al.*, 2004). The land-biosphere component, which includes parameterizations for gross photosynthesis and plant and soil respiration, is based on the model of *Eliseev and Mokhov* (2007).

As a first step, we show that when forced with historical emissions, our model is able to reproduce a variety of observations. Additionally, when forced with a suite of future emission scenarios, we find very good agreement between our predicted  $A_F$  and that obtained by the far more complex climate-carbon models participating within the Coupled Carbon Cycle Climate Model Intercomparison Project (C<sup>4</sup>MIP) experiment *Friedlingstein et al.* (2006). We next consider two families of idealized emissions, one that grows exponentially with time, and another which grows linearly. For each of these, we investigate the sensitivity of  $A_F$  to the emission growth rate. Our results suggest that the approximate constancy of the airborne fraction in the last half-century is a consequence of a nearly constant emission growth rate over that period. Furthermore, the particular value of 50-60% assumed by  $A_F$  can be explained by the exponential increase of anthropogenic emissions. If the anthropogenic emissions had been increasing linearly, for example,  $A_F$  would have achieved a much lower value. Taken together these results suggest that the (present) constancy of  $A_F$  is not a fundamental property of the carbon cycle, but depends sensitively on the emission history. Nor should we expect  $A_F$  to remain constant in the future. Fluctuations in the emission growth rate or, for Even if anthropogenic emissions continue to increase over the next century at the same exponential rate they have had since the beginning of the anthropocene,  $A_F$  would start to increase (due to a decrease in the ocean and land capacities to take up anthropogenic carbon), even in the absence of climate feedbacks. Alternatively, because of the

The paper is structured as follows. In Sec. 2 we describe the carbon model. Results of experiments designed to validate the model with anthropogenic CO<sub>2</sub> emissions based on historical data and future IPCC-SRES scenarios are presented in Sec. 3. In Sec. 4 we study the model’s response to a set of idealized emission scenarios, with the aim of understanding the factors controlling  $A_F$ . We conclude with a discussion of the main findings of this report in Sec. 5.

## 2 Model Description

We start by describing the three-box carbon cycle model that we have developed to investigate the perturbed carbon cycle. The model comprises of a well-mixed atmosphere, a land-biosphere component, and an ocean. The governing equation for the concentration of anthropogenic CO<sub>2</sub> in the atmosphere,  $C_a$ , is given by

$$\frac{d}{dt}C_a = (E_{\text{fossil}} + E_{\text{luc}}) - (F_o + F_l), \quad (1)$$

where  $t$  is time,  $E_{\text{fossil}}$  and  $E_{\text{luc}}$  are the *prescribed* emissions of anthropogenic CO<sub>2</sub> due to fossil fuel burning (including cement manufacture) and land-use change, respectively, and  $F_o$  and  $F_l$  represent the net CO<sub>2</sub> uptake by the ocean and land vegetation-soil system, respectively. (Note that we take 1765 to be the beginning of the industrial period.) To integrate this equation we require expressions for the land and ocean uptake, which we briefly describe below.

### 2.1 Terrestrial Compartment

To compute the uptake by the land biosphere we use a widely used terrestrial vegetation-soil system box model based on work by *Lenton* (2000), and modified by *Eliseev and Mokhov* (2007). The model includes representations for gross photosynthesis, and plant and soil respiration. Briefly, carbon uptake by the terrestrial vegetation-soil system is modeled as:

$$F_l = NPP - R_s, \quad (2)$$

where  $NPP$  is the terrestrial vegetation net primary production and  $R_s$  is the heterotrophic (soil) respiration, given by:

$$NPP = P - R_p$$

and

$$R_s = A_s C_s Q_{10,s}^{\frac{\Delta T_{s,g}}{\Delta T_o}},$$

where,  $P$  is the carbon production rate of photosynthesis,  $R_p$  is the autotrophic (biota) respiration rate,  $A_s$  is a constant (which is tuned to simulate the pre-industrial carbon cycle state, assumed to be in equilibrium with a value  $\text{pCO}_2^{\text{pre}} = 280$  ppm),  $C_s$  is the carbon terrestrial soil stock,  $Q_{10,s}$  is the value that serves as a multiplier for the soil-respiration value, if the global average temperature is increased by  $\Delta T_o = 10^\circ\text{C}$  and  $\Delta T_{s,g}$  is the anomaly of globally averaged annual mean surface-air temperature from a reference value. (For further details, see *Eliseev and Mokhov* (2007).) In this paper, we are not considering climate feedbacks. Thus, we set  $\Delta T_{s,g} = 0$ , and  $Q_{10,s}^{\Delta T_{s,g}/\Delta T_o} = 1$ .

### 2.2 Ocean Compartment

To model ocean uptake of anthropogenic CO<sub>2</sub>, we use the transit-time distribution (TTD) formalism (*Hall et al.*, 2004). Briefly, the flux of anthropogenic CO<sub>2</sub> into the ocean via gas exchange is given by:

$$F_o(t) = AK_{\text{ex}}(\Delta p\text{CO}_{2,a} - \Delta p\text{CO}_{2,o}), \quad (3)$$

where,  $A \sim 3.6 \times 10^{14} \text{ m}^2$  is the surface area of the ocean,  $K_{\text{ex}} \sim 0.06 \text{ mole m}^{-2} \text{ y}^{-1} \text{ ppm}^{-1}$  is the average annual global air-sea exchange coefficient from *GLODAP* (*Key et al.*, 2004),  $\Delta p\text{CO}_2$  is the anthropogenic perturbation in the partial pressure of CO<sub>2</sub>, and the subscripts ‘‘a’’ and ‘‘o’’ refer to the atmosphere and surface ocean, respectively. By mass conservation, this flux must equal the

rate of change of the total amount of anthropogenic  $\text{CO}_2$  in the ocean, i.e.,

$$F_o(t) = V \frac{d}{dt} \Delta \text{DIC}_V(t), \quad (4)$$

where,  $V \sim 1.3 \times 10^{18} \text{m}^3$  is the total volume of the ocean, and  $\Delta \text{DIC}_V$  is the unknown average concentration of anthropogenic dissolved inorganic carbon (DIC) in the ocean. Finally, to derive a prognostic equation for  $\Delta \text{DIC}_V$ , we make use of the fact that the anthropogenic perturbation is sufficiently small so as to be treated as a passive, conservative tracer. Given the time history of any such tracer in the mixed-layer, its average concentration in any interior volume is given by the convolution of the domain integrated transit-time distribution, or Green's function, with the outcrop time history (see *Hall et al.* (2004) for details). The TTD describes the complex advective-diffusive transport of tracers between the surface and the interior of the ocean. Mathematically,

$$V \Delta \text{DIC}_V(t) = \int_0^\infty \Delta \text{DIC}_s(t-t') G_V(t') dt', \quad (5)$$

where  $G_V$  is the TTD averaged over volume  $V$ , and  $\Delta \text{DIC}_s(t)$  is the concentration history averaged over the outcrop. In the present application, the domain represented by  $V$  is the global ocean. To apply the above formulation we require  $G_V(t)$  and  $\Delta \text{DIC}_s(t)$ .

Following previous work (*Hall et al.*, 2004; *Terenzi et al.*, 2007), we assume that  $G_V$  has an "inverse Gaussian" functional form, characterized by two parameters,  $\tau_M$  and  $Pe$ , which have the interpretation of a mean residence time and a Peclet number, respectively. While highly simplified, this functional form is in accord with both observations and simulations in ocean general circulation models (GCMs) (e.g., *Khatiwala et al.*, 2001). In general, there are two noteworthy limits for these parameters: the high  $Pe$  limit corresponds to bulk-advective transport (weak mixing), while the low  $Pe$  limit corresponds to diffusive transport (strong mixing). Analysis of tracer observations in the ocean (*Hall et al.*, 2004; *Waugh et al.*, 2004) strongly suggests that the weak-mixing limit is unrealistic, so we will only consider the strong mixing case. To constrain these parameters we use multiple tracers (CFC-12 and natural  $^{14}\text{C}$ ) from the GLODAP database (*Key et al.*, 2004), as described in *Waugh et al.* (2004). We find that  $Pe \sim 0.5$  and  $\tau_M \sim 2400$  years.

To obtain the surface history  $\Delta \text{DIC}_s(t)$ , we combine eqs. 3, 4, and 5, and discretize in time with annual resolution, to obtain a system of nonlinear equations for  $\Delta \text{DIC}_s(t_i)$ . Here,  $t_i$ ,  $i = 1 \dots N$ , are the times at which the continuous equation is discretized and at which the solution is desired. The nonlinearity arises from the fact that the surface  $p\text{CO}_2$  is a nonlinear function (described by the equilibrium carbonate chemistry in seawater) of the DIC concentration, for a given temperature, salinity and alkalinity. Note, too, that eq. 3 involves perturbations about the *unknown* preindustrial  $p\text{CO}_2$  of the surface ocean. Thus, this system comprises of  $N$  equations in  $N + 1$  unknowns, the additional unknown being the preindustrial surface ocean  $p\text{CO}_2$ . To eliminate the latter, we make use of surface ocean  $p\text{CO}_2$  observations (*Takahashi et al.*, 2002) at a single instance in time,  $t_{\text{obs}}$ . The resulting system is solved for  $\Delta \text{DIC}_s$  using Newton's method as described in *Terenzi et al.* (2007). Once  $\Delta \text{DIC}_s$  is known, the inventory of anthropogenic  $\text{CO}_2$  in the ocean,  $\Delta \text{DIC}_V$ , at any instant in time can be found via eq. 5. Note that our formulation does not require us to linearize the chemistry, as often done in this context when using a Green's function to characterize ocean transport. Nor do we make the assumption of constant disequilibrium. Instead, the air-sea disequi-

librium is fully allowed to evolve in time subject to the constraints of mass conservation and the observed  $p\text{CO}_{2,o}$ .

### 2.3 Method of Solution

As formulated above, to solve for the ocean and land uptake terms,  $F_o$  and  $F_l$ , respectively, we require the atmospheric  $p\text{CO}_2$  history. However, to obtain the latter we first require  $F_o$  and  $F_l$  (eq. 1). To self-consistently solve for all three components of the model, we have therefore developed an iterative procedure, as follows. We first "spin-up" the land model with a prescribed preindustrial atmospheric  $p\text{CO}_2$  concentration of 280 ppm. The resulting solution is used as an initial condition for all subsequent calculations. Second, a first guess time history of  $\Delta p\text{CO}_{2,a}$  is constructed, using historical annual mean atmospheric data from 1765 to 2004, and a suitable guess for future years depending on the kind of experimental run (see Sec. 3 and Sec. 4). Historical data are taken from OCMIP (<http://www.ipsl.jussieu.fr/OCMIP/phase2/simulations/Abiotic/boundcond/splco2.dat>), which has been updated with yearly global mean surface  $\Delta p\text{CO}_{2,a}$  from NOAA extrapolated to 2004 by adding the 5-year mean annual increase amount ([ftp://ftp.cmdl.noaa.gov/ccg/co2/trends/co2\\_annmean\\_gl.txt](ftp://ftp.cmdl.noaa.gov/ccg/co2/trends/co2_annmean_gl.txt)). Using this initial ansatz for  $p\text{CO}_{2,a}$ , we then compute a first guess for the ocean uptake,  $F_o$ . Finally, to obtain a self-consistent solution, the following steps are repeated until convergence:

- Integrate the land model with the current  $p\text{CO}_{2,a}$  iterate to obtain  $F_l$ .
- Integrate eq. 1 with current  $F_o$  and  $F_l$  iterates to obtain a new  $p\text{CO}_{2,a}$ .
- Compute new ocean uptake  $F_o$  using  $p\text{CO}_{2,a}$  computed above.

Convergence is based on the 2-norm of the difference between successive iterates of  $p\text{CO}_{2,a}$  being smaller than a given threshold. Note that in the above procedure,  $E_{\text{foss}}$  and  $E_{\text{luc}}$  are prescribed as described below.

### 3 Model Validation and Comparison With Previous Studies

To evaluate the performance of our model, we have conducted a series of experiments with anthropogenic  $\text{CO}_2$  emissions based on observations (until 2004) and IPCC-SRES emission scenarios for future years (2004-2100). To construct the historical (1765-2004) forcing, we use fossil fuel and industrial emission data from *Marland et al.* (2007), and land-use change data from *Houghton* (2008). Because the latter are available only from 1850 onward, for prior years we assume that emissions from land-use change increase linearly from 1765 to 1850, as is consistent with the observed linear trend in  $F_l$  following 1850. For the period 2004 to 2100 emissions are taken from the A2 family of the IPCC-SRES emission scenarios, specifically the ASF model ([http://sres.ciesin.columbia.edu/final\\_data.html](http://sres.ciesin.columbia.edu/final_data.html)). Since these scenarios are designed to start from a common year of 1990, we rescaled them in order to match the 2004 historical data (see Fig. 1). The combined historical and future emission time series is similar to that used in a number of recent studies (e.g., *Friedlingstein et al.*, 2006; *Eliseev and Mokhov*, 2007).

Fig. 1 shows the above emission time series, along with the

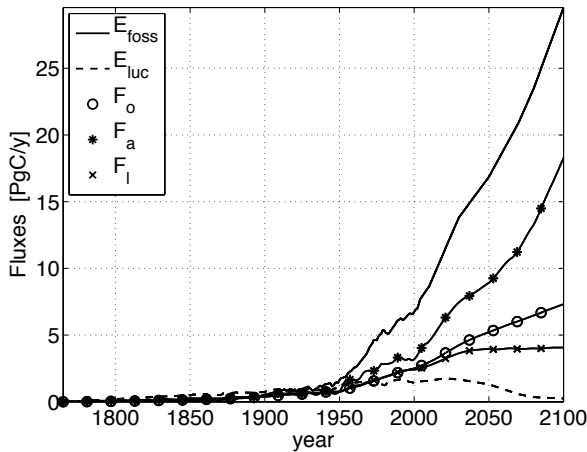


**Figure 1.** Time series of  $\text{CO}_2$  emissions ( $E_{\text{foss}}$  and  $E_{\text{luc}}$ ) used to force the model, and the resulting simulated fluxes ( $F_a$ ,  $F_o$ , and  $F_l$ ). Units are  $[\text{PgC/y}]$ .

$\text{CO}_2$  fluxes simulated by the model when forced with these emissions. Note that  $F_a$  is the rate of change of anthropogenic  $\text{CO}_2$  in the atmosphere. The anthropogenic  $\text{CO}_2$  uptake by the ocean in the model is  $F_o \sim 2.3 \text{ PgC/y}$  for the mid-1990s, which is in line with the 1.9–2.2  $\text{PgC/y}$  estimated by previous studies (Takahashi *et al.*, 2002, and references therein). The cumulative oceanic uptake of carbon dioxide for the period 1800 to 1994 in our model is  $\sim 114 \text{ PgC}$ , which is in agreement with the observational estimates of Sabine *et al.* (2004) ( $118 \pm 19 \text{ PgC}$ ) and Waugh *et al.* (2006) (94–121  $\text{PgC}$ ). The simulated terrestrial carbon uptake for 1994 is  $F_l \sim 2.3 \text{ PgC/y}$ , which is similar to previous estimates (e.g., Keeling *et al.*, 1996; Lenton, 2000). Our 116  $\text{PgC}$  simulated terrestrial inventory for 1860 to the mid-1990s falls within the range (61–141) estimated by Sabine *et al.* (2004) for the same period.

Fig. 2 compares the atmospheric  $p\text{CO}_2$  (top) and airborne fraction (bottom) simulated by the model (solid line) with observations (circles). ( $A_F$  is defined as  $F_a/(E_{\text{foss}} + E_{\text{luc}})$ .) In particular, the model reproduces well the observed atmospheric  $p\text{CO}_2$  time with a maximum error of  $\approx 8 \text{ ppm}$ . The simulated average value of  $A_F$  for the period 1900 to 2004 is  $\approx 0.4$ , which is in good agreement with the data-based estimate of Canadell *et al.* (2007), but is slightly lower than other estimates (e.g., Hansen and Sato, 2004). It is also interesting to compare our model results with those from more sophisticated carbon cycle models, and in particular the 11 models participating in the Coupled carbon cycle Climate Model Intercomparison Project ( $\text{C}^4\text{MIP}$ ) (Friedlingstein *et al.*, 2006). (Since our model lacks feedbacks between climate and the carbon cycle, we only consider the uncoupled  $\text{C}^4\text{MIP}$  simulations in which such feedbacks were switched off.) Note that, while the various  $\text{C}^4\text{MIP}$  models were forced with nominally the same IPCC-SRES A2 emission scenario, we have found slight differences between the actual emissions used to force the various models. This should be kept in mind in the following discussion. As evident from Fig. 2, our simulated  $p\text{CO}_{2,a}$  and  $A_F$  fall well within the range of values in the  $\text{C}^4\text{MIP}$  ensemble (shaded area). For instance, our predicted  $p\text{CO}_{2,a}$  for the year 2100 is 829 ppm, while the  $\text{C}^4\text{MIP}$  models range from 681–870 ppm. Similarly, for the year 2100, we predict an  $A_F$  of 0.62, compared with  $0.59 \pm 0.1$  for  $\text{C}^4\text{MIP}$ . These results indicate that our relatively simple carbon

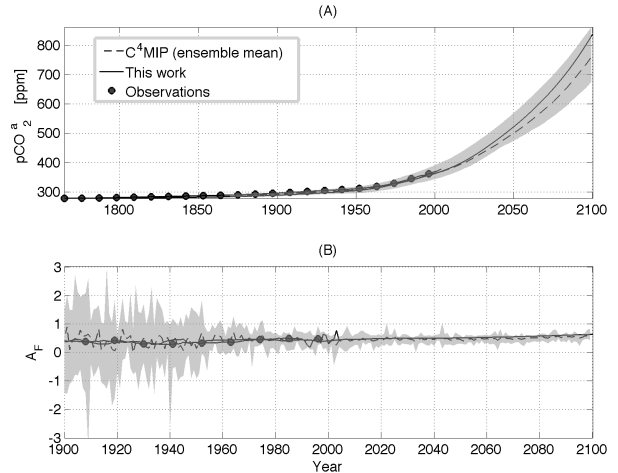


**Figure 2.** Comparison between model predictions (solid), observations (circles), and the  $\text{C}^4\text{MIP}$  ensemble means (dash) (Friedlingstein *et al.*, 2006). Top: Anthropogenic  $\text{CO}_2$  in the atmosphere [ppm]; Bottom:  $A_F$ . The shaded grey area represents the range of values encompassed by the  $\text{C}^4\text{MIP}$  models.

cycle model compares well with observations, and performs at least as well as far more sophisticated models.

## 4 Carbon Cycle Response to Idealized Emission Scenarios

Having gained confidence in the models’ ability to simulate the perturbed carbon cycle, we now address the question of what determines  $A_F$ . As mentioned earlier, the airborne fraction is considered especially relevant for climate policy, and is usually taken “as about one half” (Solomon *et al.*, 2007). Given the importance attributed to  $A_F$ , it is therefore imperative to understand the reason for the long-term constancy of the airborne fraction, and why it has stabilized around a particular value. A related question is whether a future increase in  $A_F$  necessarily imply the operation of climate-carbon feedbacks. In order to address these questions, we now consider two sets of idealized experiments with hypothetical emissions. The first experiment is designed to investigate the sensitivity of  $A_F$  to the emission history, while the second focuses on understanding recent trends in  $A_F$ .

### 4.1 Sensitivity of $A_F$ to emissions

For this experiment, we consider fossil-fuel and industry emissions only, setting emissions due to land use changes to zero. Two families of emissions are used. The first assumes an exponential behavior for  $E_{\text{foss}}$ , i.e.,  $E_{\text{foss}}(t) = E_o [\exp(\lambda(t - t_{\text{pre}})) - 1]$ , where  $E_o$  and  $\lambda$  are fit to the observed history of  $E_{\text{foss}}$ . In particular, we find a “best fit”  $\lambda$  of  $\sim (40 \text{ y})^{-1}$ . To construct the other emission curves in this family, we perturb  $\lambda$  by  $\pm 10\%$  (labeled as  $\lambda_+$  and  $\lambda_-$ , respectively). The second family of emissions we have constructed grows linearly with time, i.e.,  $E_{\text{foss}}(t) = m(t - t_{\text{pre}})$ . Three emission curves are constructed for this functional form, with the growth rate  $m$  chosen such that the cumulative emissions up to the year 2004 for each, is the same as that for the corresponding exponential curve.

The resulting  $A_F$  ( $\equiv F_a/E_{\text{foss}}$ ) and the fractions of the anthropogenic emissions that remain in the ocean ( $O_F$ ) and in the

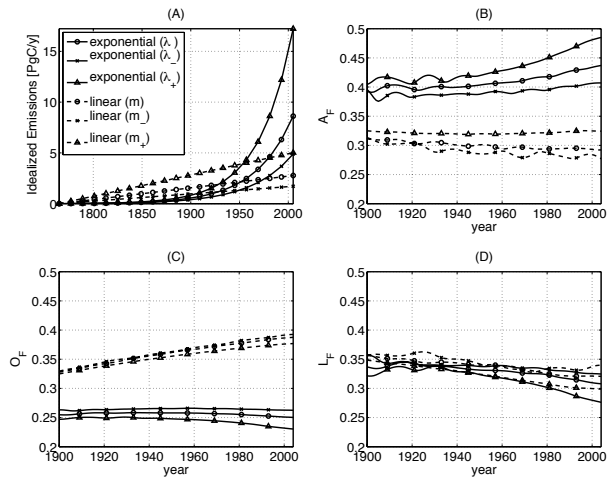


**Figure 3.** Panel (A): Hypothetical anthropogenic emissions from 1765 to 2004 in PgC/y. Solid lines represent the exponential family of emissions, while broken lines are the linear family. Panels (B), (C) and (D): simulated fractions of anthropogenic  $\text{CO}_2$  remaining in the atmosphere,  $A_F$ , in the ocean,  $O_F$ , and in the land-biosphere,  $L_F$ , for the period (1900–2004).

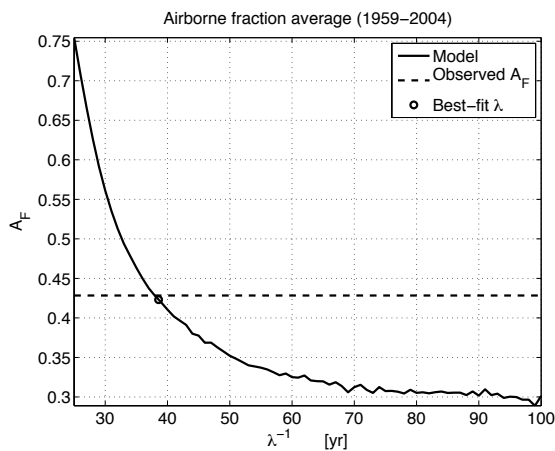


**Figure 4.** Sensitivity of  $A_F$  to exponential growth rate ( $\lambda$ ) of emissions. The solid black line represents the average value of the airborne fraction for the period 1959 to 2004 plotted against the inverse of the exponential growth rate of emissions. The horizontal broken line represents the observed value of  $A_F$  averaged over the same period. The circle represents the simulated value of  $A_F$  for  $\lambda$  that best fits the historical emission curve.

land-biosphere ( $L_F$ ) are shown in Fig. 3. (For clarity, we only plot these quantities for the period 1900 to 2004.). After a short initial transient (not shown), a quasi-constancy of  $A_F$  is achieved in all three exponential cases. The equilibrium value of  $A_F$  is not the same however, but depends on the rate of change of the emissions,  $\lambda$ . Specifically, increasing (decreasing)  $\lambda$  by 10%, increases (decreases)  $A_F$  by roughly 3–4%. The sensitivity of  $A_F$  to  $\lambda$  is shown in Fig. 4.

The response of the model to linear emissions is both qualitatively and quantitatively different. First, it takes considerably longer for the solution to approach a steady-state. Second, while the land fraction does not change appreciably, the partitioning of emissions between the ocean and atmosphere is highly sensitive to the shape of the emission curve. Specifically, the steady-state value

of  $A_F$  for exponential emissions is systematically higher than that for linear emissions. For instance,  $A_F$  for the best-fit exponential curve is about 0.43,  $\approx 30\%$  higher than that obtained using the corresponding linear emissions. Because  $L_F$  does not display much sensitivity, these differences are likely linked to the ocean uptake of anthropogenic carbon.

To understand these results, and in particular the transient behavior, we have constructed a simpler carbon model with linearized chemistry, that is much more amenable to theoretical analysis (see Appendix for details). This analysis reveals, for example, that the transient behavior of the airborne fraction is qualitatively very different for exponential and linear emissions. In particular, for exponential emissions,  $A_F$  approaches a steady state as  $\exp(\Lambda_{\min} - \lambda)t$ , where  $\Lambda_{\min}$  is the smallest eigenvalue of the linearized model. For realistic parameters, this corresponds to a time of  $O(50 \text{ y})$  to reach equilibrium. On the other hand, for linear emissions,  $A_F$  approaches equilibrium as  $t^{-1}$ , or a transient time scale of several thousand years. These results demonstrate that  $A_F$  is quite sensitive to both the shape of the emission forcing, as well as its rate of increase.

#### 4.2 Future changes assuming a “future-as-the-past” scenario

The above results show that for a fixed emission growth rate,  $A_F$  does in fact achieve a nearly constant value, at least for the period we have examined. It is not clear, however, whether this constancy will persist in the future. Indeed, some authors (e.g., *Canadell et al., 2007*) have noted a recent upward trend in  $A_F$ , and speculated that this may be evidence of a carbon-climate feedback. However, as we noted previously, the  $\text{C}^4\text{MIP}$  models in which the climate system and carbon cycle were uncoupled also show a slight increase in  $A_F$  (Fig. 2). The emission scenarios used in the  $\text{C}^4\text{MIP}$  simulations are not pure exponentials, so it is difficult to isolate the impact of a changing growth rate on  $A_F$  (cf. previous section) from other factors. To address this issue, we have carried out an additional experiment in which the model is forced by both fossil fuel and land-use change emissions. For the period 1850–2004, observed anthropogenic emissions are used, whereas for the period 2004–2100 we assume that the emissions continue to increase at the same rate as they have in the past. Specifically, future fossil fuel emissions increase exponentially, while land-use emissions increase linearly. We call this the “future-as-the-past” scenario. The exponential and linear growth rates are found by fitting those functional forms to historical data. Fig. 5 shows the simulated  $A_F$  for the period 1960–2100. As discussed previously,  $A_F$  is roughly constant until around 2000, and in good agreement with the observed value. Interestingly, the airborne fraction starts increasing after 2000, even though our model does not include any feedbacks between the climate and carbon systems. We believe that the increase in  $A_F$  can be explained simply by a decrease in the capacity of both the ocean and land-biosphere to absorb anthropogenic carbon, as evinced by decreases in both  $O_F$  and  $L_F$  (not shown). This is likely due to saturation effects such as changes in the oceanic Revelle buffer factor (e.g., *Keeling, 2005*). Indeed, when we linearize the chemistry, which in effect holds the buffer factor fixed, the upward trend disappears (not shown). Thus, even with a fixed emission growth rate, our model, with no carbon-climate feedbacks, predicts future increases in  $A_F$  because of the nonlinearity of the carbon cycle.

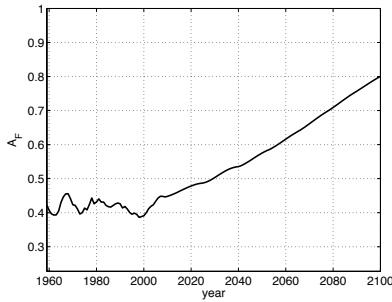


**Figure 5.** Model predicted  $A_F$  for the period 1960–2100 using the hypothetical “future-as-the-past” emissions scenario.

## 5 Conclusions

In this paper, we have presented a simple three-box model suitable for studying the anthropogenically-perturbed global carbon cycle. The model comprises of a well-mixed atmosphere, a land-biosphere component, and an ocean represented by a Green’s function. The box model reproduces well the observed atmospheric histories of  $p\text{CO}_2$  and airborne fraction, as well as the inventory and uptake rates of anthropogenic carbon by the ocean and terrestrial biosphere. Furthermore, when forced with emission scenarios from the IPCC-SRES, we generally obtain good agreement with far more sophisticated carbon cycle models. We apply this model to understand the factors controlling the airborne fraction,  $A_F$ , defined as the ratio of the annual increase of atmospheric  $\text{CO}_2$  to total emissions from anthropogenic sources. This parameter has remained roughly constant since the 1960s, which has generally been interpreted to imply that  $A_F$  is a fundamental property of the carbon cycle. Consequently, the airborne fraction is considered especially relevant for climate policy (e.g., *Firor, 1988; Solomon et al., 2007*). We find, instead, that  $A_F$  depends sensitively on the shape of the emission history and its growth rate. Specifically, our results suggest that the quasi-constancy of  $A_F$  over the past half-century is essentially a consequence of the fact that the growth rate of the historical anthropogenic emissions has not significantly changed over this period. Additionally, the particular observed average  $A_F$  value of about 50% since the 1960s can be explained by the historical emission growth rate  $\lambda$  of  $\approx(40 \text{ y})^{-1}$ . A higher (lower)  $\lambda$  would imply higher (lower)  $A_F$ . When the model is forced with linearly increasing emissions,  $A_F$  takes significantly longer to approach a steady state, and the final equilibrium value is much lower than for exponential emissions. Taken together, these results show that the airborne fraction should not be taken as a fundamental property of the carbon cycle, as previous workers have suggested (e.g., *Broecker, 1975; Broecker et al., 1979; Hansen et al., 1981; Siegenthaler and Joos, 1992; Hansen and Sato, 2004*). Furthermore, even for a fixed emission growth rate, our model predicts an increase in  $A_F$  due to changes in the absorbing capacities of the ocean (e.g., the Revelle buffer factor) and land biosphere. Thus, although we cannot rule out climate-carbon feedbacks as suggested by *Canadell et al. (2007)*, fluctuations in the emission growth rate and/or changes in the absorbing capacities of the ocean and land biosphere, offer plausible, and perhaps simpler, explanations for the recent observed trends in  $A_F$ .

## Acknowledgements

We thank Tim Hall and Jorge Sarmiento for useful discussions and comments. We also thank P. Friedlingstein and the  $\text{C}^4\text{MIP}$  community for access to their model results. This research was funded by grants xxx and xxx. LDEO contribution xxx.

## APPENDIX A: Linearized Carbon Cycle Model

In this appendix we briefly describe the linearized carbon cycle model used to understand the results of the more complex box model. In this model, the atmosphere exchanges anthropogenic  $\text{CO}_2$  with an ocean component only. The latter is represented by two boxes, a mixed layer and a deep ocean. Anthropogenic  $\text{CO}_2$  penetrates the ocean via air-sea gas exchange (eq. 3). The surface ocean, with anthropogenic DIC concentration  $\Delta\text{DIC}_s$ , in turn communicates with the deep ocean, which has a mean anthropogenic DIC concentration  $\Delta\text{DIC}_d$ . The ventilation rate is given by  $q$ . The system is described by the following equations

$$\begin{aligned} \frac{d}{dt}(m_a \Delta p\text{CO}_{2,a}) &= E_{\text{anthro}} - AK_{\text{ex}}(\Delta p\text{CO}_{2,a} - \Delta p\text{CO}_{2,o}) \\ \frac{d}{dt}(V_m \Delta\text{DIC}_s) &= q(\Delta\text{DIC}_d - \Delta\text{DIC}_s) + \\ &\quad AK_{\text{ex}}(\Delta p\text{CO}_{2,a} - \Delta p\text{CO}_{2,o}) \\ \frac{d}{dt}(V_d \Delta\text{DIC}_d) &= -q(\Delta\text{DIC}_d - \Delta\text{DIC}_s) \end{aligned} \quad (\text{A1})$$

where  $E_{\text{anthro}}$  is the anthropogenic emission,  $V_{m(d)}$  is the volume of the mixed layer (deep ocean), and  $m_a \approx 2.12 \text{ PgC/ppm}$ . To relate  $\Delta\text{DIC}_s$  to  $\Delta p\text{CO}_{2,o}$ , we exploit linearized carbonate chemistry:  $\Delta\text{DIC}_s = R\Delta p\text{CO}_{2,o} = (\frac{1}{\gamma_{\text{DIC}}})(\frac{\overline{\text{DIC}}_s}{p\overline{\text{CO}}_{2,o}})\Delta p\text{CO}_{2,o}$ . In this expression,  $\overline{p\text{CO}}_{2,o}$  and  $\overline{\text{DIC}}_s$  are the global average surface  $p\text{CO}_2$  and DIC concentration, respectively (which we take to be in a preindustrial state), and  $\gamma_{\text{DIC}} \equiv \frac{\text{DIC}}{p\text{CO}_2} \frac{\partial p\text{CO}_2}{\partial \text{DIC}}$  is the “Revelle factor”, which describes the fractional change in partial pressure of  $\text{CO}_2$  in seawater changes for a fractional change in DIC.  $\gamma_{\text{DIC}}$  is a function of sea-surface temperature (SST) and salinity (SSS). Numerical values for all parameters are given in Table A1. After introducing the time scales  $\tau_{m(d)} \equiv V_{m(d)}/q$ , eq. A1 can finally be written in matrix form as:

$$\frac{dx}{dt} = \mathbf{M}\mathbf{x} + \mathbf{F},$$

where  $\mathbf{x}$  is the vector defined as

$$\mathbf{x} = \begin{pmatrix} \Delta p\text{CO}_{2,a} \\ \Delta p\text{CO}_{2,o} \\ \Delta\text{DIC}_d \end{pmatrix},$$

$\mathbf{M}$  is the 3x3 matrix

$$\mathbf{M} = \begin{pmatrix} -\frac{AK_{\text{ex}}}{m_a} & \frac{AK_{\text{ex}}}{m_a} & 0 \\ \frac{AK_{\text{ex}}}{V_m R} & -\left(\frac{AK_{\text{ex}}}{V_m R} + \frac{1}{\tau_m}\right) & \frac{1}{R\tau_m} \\ 0 & \frac{R}{\tau_d} & -\frac{1}{\tau_d} \end{pmatrix},$$

and  $\mathbf{F}$  is the forcing vector

$$\mathbf{F}(t) = \begin{pmatrix} \widehat{E} \\ 0 \\ 0 \end{pmatrix}.$$

$\widehat{E}(t) \equiv E_{\text{anthro}}(t)/m_a$  depends on the forcing term chosen for the anthropogenic emissions. In particular, we force the model with the same exponential and linear emissions described in Sec. 4.

**Table A1.** Parameter values used in the solution of the linearized carbon cycle model.

$A$ [m <sup>2</sup> ]	$z_m$ [m]	$V_m$ [m <sup>3</sup> ]	$V_d$ [m <sup>3</sup> ]	$K_{ex}$ [mole/(m <sup>2</sup> yr ppm)]	$\gamma_{DIC}$	$q$ [m <sup>3</sup> /s]
$3.6 \times 10^{14}$	50	$1.8 \times 10^{16}$	$1.3 \times 10^{18}$	0.063	10	$20 \times 10^6$
SST [°C]	SSS [PSS]	$\overline{pCO_{2,o}}$ [ppm]	$\overline{DIC_s}$ [mole/m <sup>3</sup> ]	$ E_{exp}  \equiv E_0$ [ppm/yr]	$\tau = \lambda^{-1}$ [yr]	$ E_{lim}  \equiv m$ [ppm/yr]
15.48	34.58	280	2.06	0.0082	38.6	0.0016

**Table A2.** Eigenvalues of the matrix  $\mathbf{M}$ ,  $\Lambda_i$  [yr<sup>-1</sup>], associated time scales,  $\tau_i = \Lambda_i^{-1}$  [yr] and asymptotic values of  $A_F$  for exponential and linear anthropogenic emissions.

$\Lambda_1$	$\Lambda_2$	$\Lambda_3$	$\tau_1$	$\tau_2$	$\tau_3$	$(A_F^{lim})_{exponential}$	$(A_F^{lim})_{linear}$
-1.871	-0.003	0	-0.534	-344.441	$\infty$	0.85	0.15

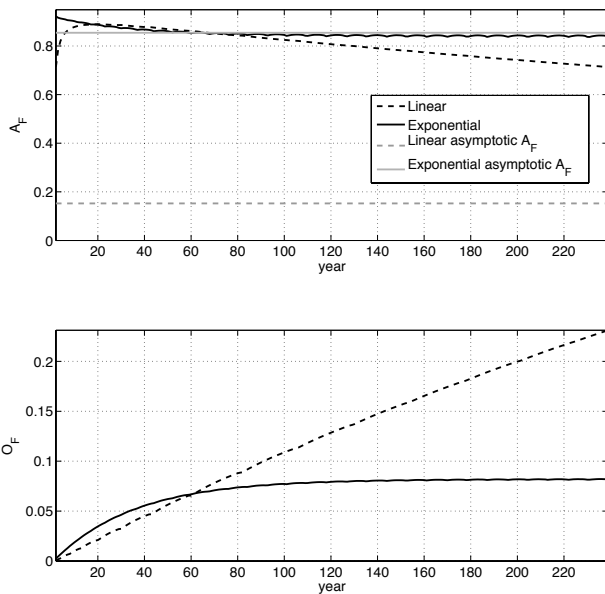

**Figure A1.** Resulting  $A_F$  (top panel) and  $O_F$  (bottom panel) from exponential (solid line) and linear (dotted line) emissions as in 4 for the simpler atmosphere-2 box ocean model. Asymptotic values for  $A_F$  for both emissions types are also plotted in grey.

Fig. A1 shows the resulting airborne and ocean fractions for the parameter values given in Table A1. Evidently, after a transient, both  $A_F$  and  $O_F$  reach asymptotic values. Also, as mentioned earlier, the time required to approach a steady state is much longer for the linear case, and the final steady state value of  $A_F$  significantly lower than for exponential emissions. This can also be seen from the following analytical expressions for  $A_F$ :

*Exponential Emissions*

$$A_F = S_{11} \left( \frac{P_{11}}{\lambda - \Lambda_1} \lambda + \frac{c_1 \Lambda_1}{E_0} e^{(\Lambda_1 - \lambda)t} \right) + S_{12} \left( \frac{P_{21}}{\lambda - \Lambda_2} \lambda + \frac{c_2 \Lambda_2}{E_0} e^{(\Lambda_2 - \lambda)t} \right) + S_{13} P_{31} \quad (\text{A2})$$

*Linear Emissions*

$$A_F = -\frac{S_{11} P_{11}}{\Lambda_1 t} + c_1 \frac{S_{11} \Lambda_1 e^{\Lambda_1 t}}{m t} - \frac{S_{12} P_{21}}{\Lambda_2 t} + c_2 \frac{S_{12} \Lambda_2 e^{\Lambda_2 t}}{m t} + S_{13} P_{31} \quad (\text{A3})$$

Here,  $c_i$  are integration constants,  $S_{ij}$  and  $P_{ij}$  are elements of the matrices  $\mathbf{S}$  and  $\mathbf{P} \equiv \mathbf{S}^{-1}$ , respectively, where  $\mathbf{S}$  is a matrix whose columns are the eigenvectors of  $\mathbf{M}$ .  $\Lambda_1$  and  $\Lambda_2$  are the (negative) eigenvalues of  $\mathbf{M}$  (the third eigenvalue is zero). Numerical values are given in Table A2.

There are several points to note about these expressions. First,  $A_F$  is a function of time for both exponential and linear emissions. Second,  $A_F$  reaches an asymptotic value as  $t \rightarrow \infty$  in both cases. In particular,  $A_F$  approaches a steady state as  $\sim e^{(\Lambda_i - \lambda)t}$  for exponential emissions, and as  $\sim t^{-1}$  for linear emissions. Therefore, the exponential case has a much shorter transient of  $O(50 \text{ y})$ , compared with the linear case ( $O(\text{several thousand years})$ ). Finally, taking the limit  $t \rightarrow \infty$  in eqs. A2 and A3 shows that the steady state value  $A_F^{lim}$  is, for realistic parameter values, always higher for exponential emissions compared with linear emissions.

## REFERENCES

- Broecker, W. S., Climatic change: Are we on the brink of a pronounced global warming?, *Science*, 189 (doi:10.1126/science.189.4201.460), 460–463, 1975.
- Broecker, W. S., T. Takahashi, H. J. Simpson, and T. H. Peng, Fate of fossil fuel carbon dioxide and the global carbon budget, *Science*, 206 (doi:10.1126/science.206.4417.409), 409–418, 1979.
- Canadell, J. G., et al., Contributions to accelerating atmospheric CO<sub>2</sub> growth from economic activity, carbon intensity and efficiency of natural sinks, *Proc. Natl. Acad. Sci. US.*, 104 (doi:10.1073/pnas.0702737104)(47), 18,866–18,870, 2007.
- Eliseev, A. V., and I. I. Mokhov, Carbon cycle climate feedback sensitivity to parameter changes of a zero-dimensional terrestrial carbon cycle scheme in a climate model of intermediate complexity, *Theor. Appl. Climatol.*, 89 (doi:10.1007/s00704-006-0260-6), 9–24, 2007.
- Firor, J., Public policy and the airborne fraction: Guest editorial, *Climatic Change*, 12, 103–105, 1988.
- Forster, P., et al., *Changes in Atmospheric Constituents and in Radiative Forcing*. Intergovernmental Panel on Climate Change (2007a). *Climate Change 2007 - The Physical Science Basis: Contribution of Working Group I to the Fourth Assessment Report of the IPCC*, Cambridge: Cambridge University Press, 2007.

- Friedlingstein, P., et al., Climate-carbon cycle feedback analysis: results from the C<sup>4</sup>MIP model intercomparison, *J. Climate*, 19 (doi:10.1175/JCLI3800.1)(14), 3337–3353, 2006.
- Fung, I. Y., S. C. Doney, K. Lindsay, and J. Jasmin, Evolution of carbon sinks in a changing climate, *Proc. Natl. Acad. Sci. U.S.*, 102 (doi:10.1073/pnas.0504949102)(32), 11,201–11,206, 2005.
- Hall, T. M., D. W. Waugh, T. W. N. Haine, P. E. Robbins, and S. Khatiwala, Estimates of anthropogenic carbon in the Indian Ocean with allowance for mixing and time-varying air-sea CO<sub>2</sub> disequilibrium, *Glob. Biogeochem. Cy.*, 18 (doi: 10.1029/2003GB002120), 2004.
- Hansen, J. E., and M. Sato, Greenhouse gas growth rates, *Proc. Natl. Acad. Sci. U.S.*, 101 (doi:10.1073/pnas.0406982101)(46), 16,109–16,114, 2004.
- Hansen, J. E., D. Johnson, A. Lacis, S. Lebedeff, P. Lee, D. Rind, and G. Russell, Climate impact of increasing atmospheric carbon dioxide, *Science*, 213 (doi:10.1126/science.213.4511.957), 957–966, 1981.
- Houghton, J. T., Y. Ding, D. J. Griggs, M. Noguer, P. J. van der Linden, X. Dai, K. Maskell, and C. A. Johnson, *Climate Change 2001: The Scientific Basis. Contribution of Working Group I to the Third Assessment Report of the Intergovernmental Panel on Climate Change*, Cambridge University Press, 2001.
- Houghton, R. A., Carbon flux to the atmosphere from land-use changes: 1850–2005. In *TRENDS: A compendium of data on global change, Data set*, Carbon Dioxide Information Analysis Center, Oak Ridge National Laboratory, U.S. Department of Energy, Oak Ridge, Tenn., U.S.A., 2008.
- Jones, C. D., and P. M. Cox, On the significance of atmospheric CO<sub>2</sub> growth rate anomalies in 2002–2003, *Geophys. Res. Lett.*, 32 (doi:10.1029/2005GL023027), L14,816, 2005.
- Joos, F., M. Bruno, R. Fink, U. Siegenthaler, T. F. Stocker, C. L. Quéré, and J. L. Sarmiento, An efficient and accurate representation of complex oceanic and biospheric models of anthropogenic carbon uptake, *Tellus B*, 48 (doi:10.1034/j.1600-0889.1996.t01-2-00006.x), 397–417, 1996.
- Keeling, C. D., T. P. Whorf, M. Wahlen, and J. V. D. Plichtt, Interannual extremes in the rate of rise of atmospheric carbon dioxide since 1980, *Nature*, 375 (doi:10.1038/375666a0), 666–670, 1995.
- Keeling, R. F., Comment on “The ocean sink for anthropogenic CO<sub>2</sub>”, *Science*, 308 (doi:10.1126/science.1109620)(5729), 1743, 2005.
- Keeling, R. F., S. C. Piper, and M. Heimann, Global and hemispheric CO<sub>2</sub> sinks deduced from changes in atmospheric O<sub>2</sub> concentration, *Nature*, 381 (doi:10.1038/381218a0), 218–221, 1996.
- Key, R. M., et al., A global ocean carbon climatology: Results from GLODAP, *Global Biogeochem. Cy.*, 18 (doi:10.1029/2004GB002247), 1–23, 2004.
- Khatiwala, S., M. Visbeck, and P. Schlosser, Age tracers in an ocean GCM, *Deep-Sea Res. I*, 48, 1423–1441, 2001.
- Lenton, T. M., Land and ocean carbon cycle feedback effects on global warming in a simple earth system model, *Tellus B*, 52 (doi:10.1034/j.1600-0889.2000.01104.x), 1159–1188, 2000.
- Marland, G., T. A. Boden, and R. J. Andres, Global, regional, and national CO<sub>2</sub> emissions. In *trends: A compendium of data on global change, Data set*, Carbon Dioxide Information Analysis Center, Oak Ridge National Laboratory, U.S. Department of Energy, Oak Ridge, Tenn., U.S.A., 2007.
- Oeschger, H., U. Siegenthaler, U. Schotterer, and A. Gugelmann, A box diffusion model to study the carbon dioxide exchange in nature, *Tellus*, 27, 168–192, 1975.
- Plattner, G. K., et al., Long-term climate commitments projected with climate-carbon cycle models, *J. Climate*, 21 (doi:10.1175/2007JCLI1905.1), 2721–2751, 2008.
- Sabine, C. L., et al., The ocean sink for anthropogenic CO<sub>2</sub>, *Science*, 305 (doi:10.1126/science.1097403)(5682), 367–371, 2004.
- Sarmiento, J. L., and J. R. Toggweiler, New model for the role of the oceans in determining atmospheric pCO<sub>2</sub>, *Nature*, 308 (doi:10.1038/308621a0), 621–624, 1984.
- Siegenthaler, U., and F. Joos, Use of a simple model for studying oceanic tracer distributions and the global carbon cycle, *Tellus B*, 44 (doi:10.1034/j.1600-0889.1992.t01-2-00003.x), 186–207, 1992.
- Siegenthaler, U., and H. Oeschger, Predicting future atmospheric carbon dioxide levels, *Science*, 199 (doi:10.1126/science.199.4327.388)(4327), 388–395, 1978.
- Solomon, S., D. Qin, M. Manning, M. Marquis, K. Averyt, M. M. B. Tignor, H. L. M. Jr., and Z. Chen, *Intergovernmental Panel on Climate Change (2007a). Climate Change 2007 - The Physical Science Basis: Contribution of Working Group I to the Fourth Assessment Report of the IPCC*, Cambridge: Cambridge University Press, 2007.
- Takahashi, T., et al., Global sea-air CO<sub>2</sub> flux based on climatological surface ocean pCO<sub>2</sub>, and seasonal biological and temperature effects, *Deep-Sea Res. Pt. II*, 49 (doi:10.1016/S0967-0645(02)00003-6), 1601–1622, 2002.
- Terenzi, F., T. M. Hall, S. Khatiwala, C. B. Rodehacke, and D. A. LeBel, Uptake of natural and anthropogenic carbon by the Labrador Sea, *Geophys. Res. Lett.*, 34 (doi: 10.1029/2006GL028543), 2007.
- Toggweiler, J. R., A. Gnanadesikan, S. Carson, R. Murnane, and J. L. Sarmiento, Representation of the carbon cycle in box models and GCMs: 1. Solubility pump, *Global Biogeochem. Cy.*, 17 (doi:10.1029/2001GB001401), 26.1–26.11, 2003a.
- Toggweiler, J. R., A. Gnanadesikan, S. Carson, R. Murnane, and J. L. Sarmiento, Representation of the carbon cycle in box models and GCMs: 2. Organic pump, *Global Biogeochem. Cy.*, 17 (doi:10.1029/2001GB001841), 27.1–27.13, 2003b.
- Waugh, D. W., T. W. N. Haine, and T. M. Hall, Transport times and anthropogenic carbon in the subpolar North Atlantic Ocean, *Deep-Sea Res. Pt. I*, 51 (doi:10.1016/j.dsr.2004.06.011), 1475–1491, 2004.
- Waugh, D. W., T. M. Hall, B. I. McNeil, R. M. Key, and R. J. Matear, Anthropogenic CO<sub>2</sub> in the oceans estimated using transit-time distributions, *Tellus B*, 58 (doi:10.1111/j.1600-0889.2006.00222.x), 376–390, 2006.